Investigation of dissolution rate kinetics of bulk pharmaceutical feed streams within a stirred tank vessel and a twin screw extruder

Investigation of dissolution rate kinetics of bulk pharmaceutical feed streams within a stirred tank vessel and a twin screw extruder

Arabella M McLaughlin, John Robertson & Xiong-Wei Ni

Investigation of dissolution rate kinetics of bulk pharmaceutical feed streams within a stirred tank vessel and a twin screw extruder

Arabella M McLaughlin[a], John Robertson[b] and Xiong-Wei Ni[a]*

[a]EPSRC Centre for Continuous Manufacturing and Crystallisation (CMAC), Centre for Oscillatory Baffled Reactor Applications (COBRA), School of Engineering and Physical Science, Heriot-Watt University, Edinburgh, EH14 4AS, UK

[b]EPSRC Future Continuous Manufacturing and Advanced Crystallisation Research Hub, University of Strathclyde, Technology and Innovation Centre, 99 George Street, Glasgow, G1 1RD, U.K.

*the corresponding author, tel: 00441314513781; fax: + 441314513129; email:

x.ni@hw.ac.uk

Investigation of dissolution rate kinetics of bulk pharmaceutical feed streams within a stirred tank vessel and a twin screw extruder

The introduction of continuous manufacturing of pharmaceuticals has highlighted the challenging area of continuous dissolution of solids for work ups to flow chemistry systems. In this study, the use of a 16mm twin screw extruder (TSE) as a platform technology for solid feeds is investigated using four solid pharmaceutical ingredients (PI) in a mixture of water and IPA. In order for comparison, the same experiments were also carried out in a batch traditional stirred tank vessel (STV). The objectives of this work are to gain further scientific understanding on dissolution kinetics and to compare kinetics in both a batch and continuous system. The concentration of each PI during dissolution is monitored using an in-line UV-ATR probe, allowing the extraction of dissolution kinetics. Faster dissolution rates are achieved in the TSE than in the STV due to higher power dissipation generated by the aggressive shear mixing and thermal energy within the TSE. Complete dissolution of paracetamol is obtained within the residence time of the TSE; complete dissolution of benzoic acid and acetylsalicylic acid are achieved at higher barrel temperatures; however full dissolution of nicotinic acid is not achievable in the TSE under the experimental conditions.

Keywords: dissolution, solid dosing, kinetics, continuous pharmaceutical manufacture, twin screw extruder and UV spectrometry.

Introduction

Active pharmaceutical ingredient (API) manufacturing is mostly conducted in batch mode where chemical ingredients and solvents are charged to a reaction vessel, a chemical reaction performed, separation unit operations conducted such as extraction or filtration, the product is then crystallised, and finally isolated by filtration and drying. The development of an efficient flow process is often the result of designing and implementing a new concept or piece of equipment that is better suited to performing an otherwise challenging task (Baumann and Baxendale 2015). Continuous processing can generally be conceptualised by several reactions and separation unit operations running

simultaneously, with constant flow of materials in and out of each reactor or separator.

Continuous processing in the pharmaceutical industry has gained significant attractions recently as it offers potential flexibility, quality and economic advantages over batch operation (Ni 2006; McGlone et al. 2015; O'Connor and Lee 2017). Substantial research in reaction, crystallisation and filtration have been reported in the past decade (Simon Lawton 2009,; Ferguson et al. 2013; Salvatore et al. 2013; Bernhard et al. 2015; Besenhard et al. 2017), however, continuous work up, e.g. solid dissolution and dosing, remains a challenging area yet to be addressed (Cole and Johnson 2018) with problems in maintaining slurry homogeneity in flow and in blocking valves and nozzles during downstream processing when solids are present (Hughes 2018).

The introduction of raw materials and intermediates for continuous pharmaceutical manufacturing processes are currently based on batch feed methodology, e.g. using stirred tank vessels for dissolution of solid particles (Wood 2009; Hörmann et al. 2011). Depending on the physical properties of the solids, such as non-wetting (hydrophobic), cohesive or adhesive, dissolution of solids in batch vessels is often a labour intensive and time consuming operation. Moreover, it is accompanied by common problems involving mass transfer limitation for solids dissolution, non-uniformity of slurry composition on discharge, and nozzles plugged by solids. If solids are cohesive there is potential for agglomeration. For adhesive solids accumulation on the impellers, baffles and supports occur readily. This leads to batch to batch variations on product quality.

Continuous processing can be thought of as the constant pumping of one or more reagent solutions into and product out of a reactor. One aspect of continuous processing for which little progress has been made concerns the way in which reagents streams are delivered into the reactors. Early investigations into flow chemistry focused

on the delivery of liquid streams. This was achieved using syringe pumps, piston pumps or rotary pumps. Unfortunately syringe pump applications are significantly limited by relatively low working pressures and often needed manual intervention when recharging the syringe. Both piston and rotary pumps suffer from inaccurate flow rates and fouling due to their direct interactions with the chemicals being pumped. In addition, both pumping solutions must be homogeneous. Slurries can cause immense complications. Hence, these technologies cannot provide consistent and accurate control of reagent to flow reactors.

In order to address these issues, flow equipment has instead been based on peristaltic pumps. An early application of such a system for commercial use was reported in 2013 by the Ley group with their continuous synthesis of an important anticancer agent tamoxifen (Murray et al. 2013). The pump design allowed a smooth and consistent delivery of a solution drawn directly out of the supplier's reagent bottle.

In 2014 researchers from Eli Lilly (US) evaluated flow techniques in which peristaltic pumps were used to direct solutions via a static mixer into a plug flow reactor (Polster et al. 2014). However, the reagent solutions were prepared in situ in a batch vessel prior to delivery to the continuous flow reactor.

A continuous solid dosing system incorporating complete dissolution would overcome the above issues. Twin screw extruders have extensively been studied for hot melt extrusion (Crowley et al. 2007; Repka et al. 2007; Patil et al. 2015; Martinez-Marcos et al. 2016) and wet granulation (Dhenge et al. 2011; Dhenge et al. 2012; Vercruysse et al. 2012; Cartwright et al. 2013; Saleh et al. 2015; Mendez Torrecillas et al. 2017). Our previous work highlighted the twin screw extruder as a potential platform for continuous delivery of solids to a flow process (McLaughlin Arabella M. et al. 2018). The objectives of this work are to further investigate continuous solid dosing and

dissolution using four solid PIs (acetylsalicylic acid, benzoic acid, nicotinic acid, and paracetamol) of varying physical and chemical properties as well as flowability; to gain scientific understanding on dissolution kinetics and to compare kinetics between batch and continuous operations.

Materials and Methods

Materials

The solvent composition used in this study was a water/IPA (80:20) mixture. Propan-2-ol (IPA) (>99.5% purity) was sourced from Sigma-Aldrich (Gillingham, UK). Deionised water was produced using the in-house Millipore Milli-Q system.

Acetylsalicylic acid (white powder with purity $\geq$99.0%), benzoic acid (white crystalline powder with purity $\geq$99.5%) and nicotinic acid (white powder with purity $\geq$98%) were supplied by Merck. Paracetamol (white powder of 99% purity) was supplied by Mallinckrodt Chemical Limited (UK).

The mean particle size and particle size distributions (see Figure 1) were analysed by a Mastersizer (HYDRO, Malvern 3000). Five measurements were taken, and the average values are given in Table 1. The samples were dispersed in hexane and added directly to the particle sizer. We see that benzoic acid has the largest mean size, while nicotinic acid the smallest.

Methods

Scanning Electron Microscopy (SEM) Analysis

SEM analysis was carried out for each PI using a Quanta 3D FEG and is presented in Figure 2, where benzoic acid is off flake shape, while acetylsalicylic acid is the column shaped.

These materials have a range of polarity, hydrogen bonding ability and solubility as shown in Table 2 (Source: PubChem, URL: *https://pubchem.ncbi.nlm.nih.gov*, Description: Data deposited in or computed by PubChem).

Solubility

Solubility of each PI in a 100g of water/IPA (80:20) mixture has been determined by a gravimetric method.

Stirred Tank Vessel (STV)

The stirred tank vessel consists of a jacketed glass vessel of 1 litre in volume, with a PTFE four-blade pitched impeller to generate mixing (see Figure 3). The impeller was attached to an overhead motor to control the rotation speeds. The vessel was fitted with a 5 port PTFE lid which enables the insertion of PAT probes and the dosing funnels. Temperature within the vessel was achieved by controlling the jacket temperature using a water bath (Grant Instruments GP 200/R2). UV-ATR and temperature (PT100) probes were inserted into the vessel to monitor and record the solute concentration and temperature of the solution during dissolution. The system was interfaced with a Carl Zeiss MC600 Spectrometer and PC for real-time display, logging and data analysis. The UV spectra were collected continuously over the spectral range of 190 – 280nm, using Aspect Plus software from Carl Zeiss. The PAT probes also act as the baffles in the STV.

For each experimental run, 1000g of solvent was added to the STV and heated/cooled to the desired temperature (40°C), 63g of PI was weighed using an electronic balance and was poured into the vessel using a funnel in order to minimise loss, giving a target solution concentration of 6.3 g (solute)/100 g (solvent). The solution was held at temperature and stirred under a fixed rotational speed - 500 rpm

(maximum speed achievable without excessive splashing and vortexing) until dissolution was complete isothermally. Solute concentration was measured, and dissolution rates determined.

Twin Screw Extruder (TSE)

A 16mm diameter twin screw extruder (Eurolab 16, Thermo Fisher Scientific, Stone, UK) is shown in Figures 4 and 5. The barrel has a length of 400 mm with a length to diameter ratio of 25:1. Liquids are dispensed into the barrel using a peristaltic pump (Watson Marlow, Falmouth, UK) and solids added via a loss in weight (LIW) gravimetric feeder, in this way, the liquid feed is decoupled from the solid input, enabling feeds of materials of two phases simultaneously. Two types of solid feeders were used in this work including a Brabender MT-S LIW Feeder and a Brabender FW-18 Flexwall Classic LIW Feeder. The former is a rigid frame laboratory scale feeder with twin concave screws suitable for low feed rates of high bulk density materials (e.g. benzoic acid and acetylsalicylic acid), while the latter is a universal flexible wall feeder with a single spiral screw suitable for materials with poor flowability and low bulk density (e.g. powder paracetamol and nicotinic acid).

The extruder was connected to a central control unit where temperature and screw speed can be varied. The temperatures of different sections along the barrel were controlled by electrical heating bands and monitored by thermocouples, enabling either different temperature profiles or isothermal condition along the barrel. A bespoke discharge coupling, and tubing connected to the twin screw exit provides downward output of material. This prevents build-up of material at the extruder exit. The UV-ATR probe was mounted on a retort stand and inserted into the tubing. Absorbance data was collected continuously using the UV-ATR probe inserted at the flow exit, interfaced with a Carl Zeiss MC600 Spectrometer and a PC for real-time display, logging and data

analysis. From which concentration profiles of PI solute in the water/IPA (80:20) solvent were established using a pre-determined calibration curve. The residence time of liquid within the barrel was measured to determine dissolution kinetics. A dye was injected at the liquid input and the minimum residence time recorded. When liquid enters the barrel at port 6, the residence time is merely 3 seconds, which is the same as the UV probe capture time, hence the UV probe is insufficient to allow direct measurement for this case, a digital stopwatch was used instead. The variation obtained was $\pm$ 0.2 seconds for five measurements.

In dissolution work, solids are dosed at Port 1 of the barrel as shown in Figure 6. Liquid flows from the right to left and can be pumped in at any of the Ports from 2 to 6 (see Figure 6). In this way, the decoupling of the dry solids from the wet liquid is achieved, preventing solids from sticking around the feeder. Liquid coming in at Port 2 has the longest residence time of 13 seconds within the barrel whereas liquid at Port 6 the shortest residence time of 3 seconds. The PI was continuously dosed into the TSE using the LIW feeder at a feed rate of 2.5 g min-1 and the solvent (Water/IPA 80:20) at a flow rate of 40 g min-1, giving a target solution concentration of 6.3 g (solute)/100 g (solvent). This is equivalent to the target concentration in the STV.

In order to obtain a concentration-time profile, calibration curves of absorbance versus concentration were generated from known amounts of PI in the Water/IPA (80:20) solvent system. A complete set of sequential runs were then undertaken at each port, e.g. Run 1 at Port 6, Run 2 at Port 5, Run 3 at Port 4, and so on. This enabled monitoring of the dissolution process along the length of the barrel. The absorbance measurements were recorded using the in-line UV-ATR probe positioned at the TSE exit. Compiling the output concentrations at each port, a dissolution profile was finally assembled.

Solvent composition has previously been identified as a factor influencing the dissolution rate, therefore the same composition was used in both the twin screw extruder and the stirred tank vessel; the mass of solute required for the lowest stable solid feed rate in the former was adopted by both systems, while the mass of solvent was calculated to allow the same theoretical solution concentration in both systems.

Results and Discussion

Calibrations

Calibration curves were generated by measuring the absorbance of known amounts of each PI in water/IPA (80:20) at 40˚C, (see supplementary material); these were subsequently used to determine the concentration of solute in solution for each dissolution test. Maximum absorbance peak was 248 nm for paracetamol, 197 nm for benzoic acid, 199 nm for acetylsalicylic acid and 193 nm for nicotinic acid.

Solubility

It has been noted that benzoic acid and acetylsalicylic acid are aromatic carboxylic acids, nicotinic acid is a pyridine carboxylic acid and paracetamol is a class of phenols (4-aminophenol in which one of the hydrogens attached to the amino group has been replaced by an acetyl group). The aromatic carboxylic acids have the lowest solubility in water (see Table 2), while the pyridine carboxylic acid and the amino phenol classes have greater solubility due to the nitrogen atom in their chemical structure. The increased hydrogen bonding ability of acetylsalicylic acid which has 4 hydrogen bond acceptors enables greater solubility in water than benzoic acid which has 2 hydrogen bond acceptors. This is also the case for nicotinic acid which has 3 hydrogen bond acceptors whereas paracetamol has 2 and lower solubility in water than nicotinic acid. These are reflected in the solubility graph in Figure 7 where a water/IPA (80:20)

mixture is the solvent. Paracetamol has the highest solubility, with nicotinic acid having the lowest solubility.

Figure 7 also shows the effect of temperature on solubility for each PI. The solution process absorbs energy and the solubility increases as the temperature increases, for benzoic acid however, the solubility profile is rather different from the rest, which is consistent with previously published work by Humayun (Humayun et al. 2016).

Dissolution tests

Dissolution tests were performed in triplicate using the four PIs in turn. These tests were executed in both the STV and in the TSE using the method conditions as described in the Methods section above.

Dissolution in STV

Figure 8 shows the dissolution profiles for paracetamol, benzoic acid, acetylsalicylic acid and nicotinic acid. Three runs were carried out for each PI in the dissolution tests to ensure good repeatability as illustrated in Figure 9. Equilibrium solubility at 40°C is given in Table 3.

The initial concentrations from the dissolution profiles (up to the plateau) were used to extract the dissolution kinetics. The straight line fit in the plots of ln (C2/C1) vs time confirmed the first order kinetics and the slope of which gives the rate constant of dissolution *k* as shown in Table 4, where C2 and C1 are the concentrations of PI (g 100g-1) at the starting and dissolution times.

The PI materials have different wetting characteristics which affects both the time to wet the material and the time to achieve dissolution. The time to wet was 3 seconds for paracetamol, 6 seconds for nicotinic acid, 6 seconds for benzoic acid and 9

seconds for acetylsalicylic acid; the subsequent dissolution time is 42 seconds for paracetamol, 21 seconds for nicotinic acid, 93 seconds for acetylsalicylic acid and 189 seconds for benzoic acid. The faster dissolution rates for paracetamol and nicotinic acid are comparable to previous work (McLaughlin Arabella M et al. 2018) where powders with narrow particle size distribution (see Figure 1) and small particle size (see Table 1) enhanced the dissolution rate due to larger surface area. Conversely, benzoic acid and acetylsalicylic acid have broad particle size distribution and larger particles which contribute their slower dissolution rates. Note that for 63 g of PI in 1000 g of solvent, paracetamol was an unsaturated solution, while benzoic acid, acetylsalicylic acid and nicotinic acid a supersaturated solution. These would affect the dissolution and will be discussed later. The UV probe response time for the absorbance data was 3 seconds, by reducing the mass of solute to allow all solutions undersaturated would result in insufficient data collation for paracetamol and nicotinic acid that have fast initial dissolution rates, i.e. less than 9 seconds.

Dissolution in Twin Screw Extruder

A complete set of sequential runs were undertaken for liquid entering at each port, e.g. Run 1 at Port 6, Run 2 at Port 5, Run 3 at Port 4, and so on. Compiling the output concentrations at each port, the dissolution profiles were finally assembled in Figure 10. Note that each concentration measurement was repeated 3 times and the data in Figure 10 are the averaged value from three repeats. Error bars are not shown on the graph as they are too small to see clearly. The averaged standard error was 0.1.

Figure 10 shows that complete dissolution was obtained within the residence time of the barrel (14 seconds) for paracetamol where the concentration at the exit was 6.2 g per 100 g solvent. Benzoic acid, acetylsalicylic acid and nicotinic acid did not fully dissolve within the residence time of the barrel with the concentration at exit of 4.1

g, 2.2 g, and 2.3 g per 100 g solvent, respectively. This is consistent with the dissolution tests in the STV however the dissolution is faster in the TSE as the time taken to wet and dissolve particles is overcome by mechanical forces in the TSE.

Dissolution Kinetics

The rate constant of dissolution k was determined using the same methodology as used in STV, the comparison of the dissolution rate constants are given in Table 4.

We used 63 g of PI in 1000 g of solvent as the basis for comparison because this was the lowest solid flow rate for the TSE. At these fixed solid and liquid feed rates and based on the solubilities of the PIs, it resulted in an undersaturated solution for paracetamol and supersaturated solutions for benzoic acid, acetylsalicylic acid and nicotinic acid, as shown in Table 5. These would affect the dissolution rates and the degree of saturation was taken into account; the dissolution rate constants of benzoic acid, acetylsalicylic acid and nicotinic acid were recalculated by extrapolation with respect to the same undersaturation of paracetamol assuming a linear relationship in solubilities and re-tabulated in Table 5.

We can now see that the dissolution rates are similar for each material in the stirred tank, however much more aggressive local shear mixing and higher thermal energy generated by the rotation of the screws (Thiry et al. 2015) had a greater impact on disintegrating the particles and enhancing the dissolution rates in the TSE. This also delivers good uniformity of the solute in the solution. In terms of dissolution time, it took 14 seconds to dissolve 62g of paracetamol in the TSE vs 42 seconds in the stirred tank vessel to dissolve the same amount of PI. Dissolution within the short residence time of the TSE is feasible for slowly dissolving materials. The dissolution rate can be enhanced by increasing the barrel temperature using predictions from the solubility curves.

Achieving complete dissolution in the twin screw extruder

From Figure 10, we see that complete dissolution was not achievable at these solid feed rates for benzoic acid, acetylsalicylic acid and nicotinic acid. Further tests were undertaken to determine if a completely dissolved solution could be obtained on exit from the TSE which could then be fed into downstream flow processes. From the solubility graph in Figure 7, increasing the solution temperature enables fuller dissolution. Previous studies have shown that increasing the barrel temperature within the TSE is an effective way to improve dissolution of the output solution. Complete dissolution was attained for benzoic acid and acetylsalicylic acid when the temperature of the output solution increased from 40 to 50 ˚C, by increasing the barrel temperature, as shown in Figure 11.

At the solution temperature of 50 ˚C, however, complete dissolution of nicotinic acid was still not reachable. Our previous work (McLaughlin Arabella M. et al. 2018) demonstrated that operational parameters, including liquid flow rate, solid feed rate, screw speed, screw configuration and barrel temperature, can also affect dissolution rate within the TSE, but none of the above resulted in complete dissolution within the residence time of the barrel, instead a slurry was obtained with good homogeneity, e.g. the error of mass balance between the input and exit was 0.49 % RSD. This slurry can also be fed into continuous flow processes as it has consistent concentration.

Conclusions

In this work, the feasibility of using the twin screw extruder for continuous delivery of solids was examined using four solid PIs. Full dissolution of powder paracetamol was attained within the residence time of the TSE, while full dissolution of benzoic acid and acetylsalicylic acid was achieved at higher barrel temperature. These subsequent

solutions can then be fed into any pharmaceutical downstream processes. Full dissolution of nicotinic acid was not achievable in the TSE under the experimental conditions, a slurry of good homogeneity was obtained.

The dissolution rate in the TSE is faster than that in the STV, associating with higher power dissipation generated by the aggressive shear mixing and thermal energy within the barrel.

The major advantages of using the twin screw extruder as continuous dissolution of solid material for delivering solids to flow processes are it enables the decoupling of liquid from the solid feed thus eliminating any potential fouled solid feeding. The significance of this is that there is a reduced potential of variations in solution quality and the continuous equipment is less likely to stop the flow of materials in and out due to blockages, and the ability of using low solid feed rates, 2.5 g min^{-1}, with consistent dissolution concentration.

Declaration of Interest Statement

The authors report no conflicts of interest.

References

Baumann M, Baxendale IR. 2015. The synthesis of active pharmaceutical ingredients (APIs) using continuous flow chemistry. Beilstein Journal of Organic Chemistry. 11:1194-1219.

Bernhard G, David C, Oliver KC. 2015. Continuous-Flow Technology—A Tool for the Safe Manufacturing of Active Pharmaceutical Ingredients. Angewandte Chemie International Edition. 54(23):6688-6728.

Besenhard MO, Neugebauer P, Scheibelhofer O, Khinast JG. 2017. Crystal Engineering in Continuous Plug-Flow Crystallizers. Crystal Growth & Design. 17(12):6432-6444.

Cartwright JJ, Robertson J, D'Haene D, Burke MD, Hennenkamp JR. 2013. Twin screw wet granulation: Loss in weight feeding of a poorly flowing active pharmaceutical ingredient. Powder Technology. 238:116-121.

Cole KP, Johnson MD. 2018. Continuous flow technology vs. the batch-by-batch approach to produce pharmaceutical compounds. Expert Review of Clinical Pharmacology. 11(1):5-13.

Crowley MM, Zhang F, Repka MA, Thumma S, Upadhye SB, Battu SK, McGinity JW, Martin C. 2007. Pharmaceutical applications of hot-melt extrusion: part I. Drug development and industrial pharmacy. 33(9):909-926.

Dhenge RM, Cartwright JJ, Doughty DG, Hounslow MJ, Salman AD. 2011. Twin screw wet granulation: Effect of powder feed rate. Advanced Powder Technology. 22(2):162-166.

Dhenge RM, Cartwright JJ, Hounslow MJ, Salman AD. 2012. Twin screw wet granulation: Effects of properties of granulation liquid. Powder Technology. 229:126-136.

Ferguson S, Morris G, Hao HX, Barrett M, Glennon B. 2013. Characterization of the anti-solvent batch, plug flow and MSMPR crystallization of benzoic acid [Article]. Chemical Engineering Science. 104:44-54. English.

Hörmann T, Suzzi D, Khinast JG. 2011. Mixing and Dissolution Processes of Pharmaceutical Bulk Materials in Stirred Tanks: Experimental and Numerical Investigations. Ind Eng Chem Res. 50(21):12011-12025.

Hughes DL. 2018. Applications of Flow Chemistry in Drug Development: Highlights of Recent Patent Literature. Organic Process Research & Development. 22(1):13-20.

Humayun HY, Shaarani MNNM, warrior A, Abdullah B, Salam MA. 2016. The Effect of Co-solvent on the Solubility of a Sparingly Soluble Crystal of Benzoic Acid. Procedia Engineering. 148:1320-1325.

Martinez-Marcos L, Lamprou DA, McBurney RT, Halbert GW. 2016. A novel hot-melt extrusion formulation of albendazole for increasing dissolution properties. International journal of pharmaceutics. 499(1):175-185.

McGlone T, Briggs NEB, Clark CA, Brown CJ, Sefcik J, Florence AJ. 2015. Oscillatory Flow Reactors (OFRs) for Continuous Manufacturing and Crystallization. Organic Process Research & Development. 19(9):1186-1202.

McLaughlin AM, Robertson J, Ni X-W. 2018. On the Use of a Twin Screw Extruder for Continuous Solid Feeding and Dissolution for Continuous Flow Processes. Organic Process Research & Development.

McLaughlin AM, Robertson J, Ni X. 2018. Material characterisation and parameter effects on bulk solid dissolution rate of paracetamol in a stirred tank vessel using an in situ UV-ATR probe. International Journal of Engineering Research & Science. 4(1):10-20.

Mendez Torrecillas C, Halbert GW, Lamprou DA. 2017. A novel methodology to study polymodal particle size distributions produced during continuous wet granulation. International journal of pharmaceutics. 519(1):230-239.

Murray PRD, Browne DL, Pastre JC, Butters C, Guthrie D, Ley SV. 2013. Continuous Flow-Processing of Organometallic Reagents Using an Advanced Peristaltic Pumping System and the Telescoped Flow Synthesis of (E/Z)-Tamoxifen. Organic Process Research & Development. 17(9):1192-1208.

Ni X. 2006. Continuous Oscillatory Baffled Reactor Technology. Innovations in Pharmaceutical Technology. 20:90-96.

O'Connor T, Lee S. 2017. Chapter 37 - Emerging Technology for Modernizing Pharmaceutical Production: Continuous Manufacturing A2 - Qiu, Yihong. In: Chen Y, Zhang GGZ, Yu L et al., editors. Developing Solid Oral Dosage Forms (Second Edition). Boston: Academic Press; p. 1031-1046.

Patil H, Tiwari RV, Repka MA. 2015. Hot-Melt Extrusion: from Theory to Application in Pharmaceutical Formulation. AAPS PharmSciTech.

Polster CS, Cole KP, Burcham CL, Campbell BM, Frederick AL, Hansen MM, Harding M, Heller MR, Miller MT, Phillips JL et al. 2014. Pilot-Scale Continuous Production of LY2886721: Amide Formation and Reactive Crystallization. Organic Process Research & Development. 18(11):1295-1309.

Repka MA, Battu SK, Upadhye SB, Thumma S, Crowley MM, Zhang F, Martin C, McGinity JW. 2007. Pharmaceutical applications of hot-melt extrusion: Part II. Drug development and industrial pharmacy. 33(10):1043-1057.

Saleh MF, Dhenge RM, Cartwright JJ, Hounslow MJ, Salman AD. 2015. Twin screw wet granulation: Binder delivery. International journal of pharmaceutics. 487(1–2):124-134.

Salvatore M., Heider. P. L., Haitao, Z., Lakerveld, R., Brahim, B., Barton, P. I., Braatz, R. D., Cooney, C. L., Evans, J. M. B., Jamison, T. F., Jensen, K.F., Myreson, A.S., Trout,B.L.2013. End-to-End Continuous Manufacturing of Pharmaceuticals: Integrated Synthesis, Purification, and Final Dosage Formation. Angewandte Chemie International Edition. 52(47):12359-12363.

Simon Lawton GS, Phil Shering. 2009,. Continuous Crystallization of Pharmaceuticals Using a Continuous OscillatoryBaffled Crystallizer. Organic Process Research & Development. 13:1357–1363.

Thiry J, Krier F, Evrard B. 2015. A review of pharmaceutical extrusion: critical process parameters and scaling-up. International journal of pharmaceutics. 479(1):227-240.

Vercruysse J, Córdoba Díaz D, Peeters E, Fonteyne M, Delaet U, Van Assche I, De Beer T, Remon JP, Vervaet C. 2012. Continuous twin screw granulation: Influence of process variables on granule and tablet quality. European Journal of Pharmaceutics and Biopharmaceutics. 82(1):205-211.

Wood A. 2009. Generic Batch Procedures for Flexible Manufacturing [Article]. Control Engineering. 56(3):P1-P5.

Word Count = 4750 words
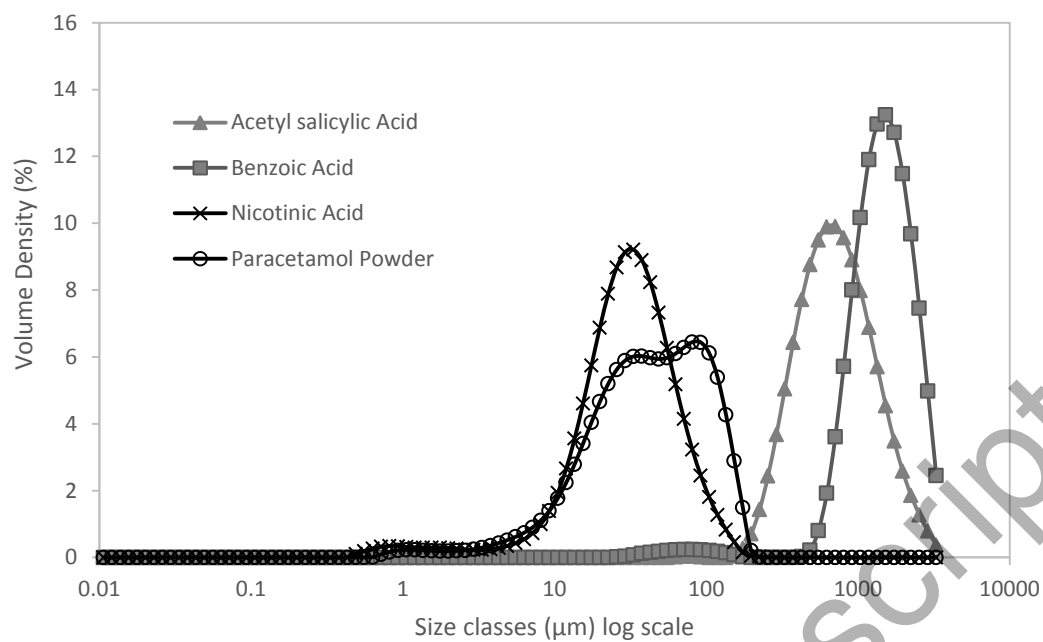
Figures

Figure 1 Particle size distribution of acetylsalicylic acid, benzoic acid, nicotinic acid and paracetamol using laser diffraction

(a)   (b)

(c)   (d)
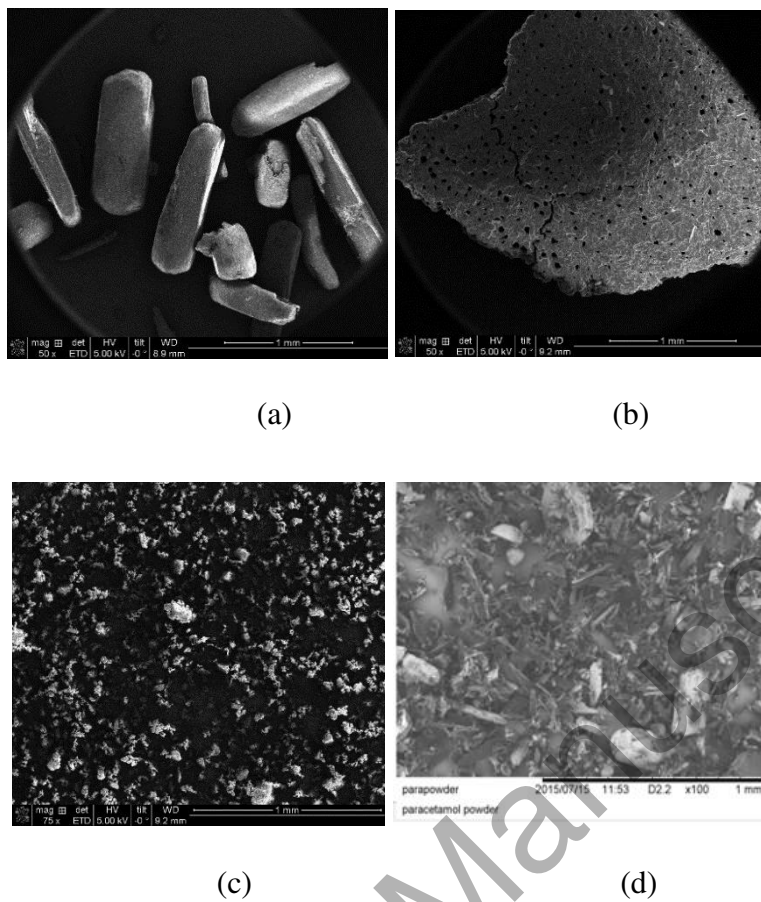
Figure 2 SEM images of (a) Acetylsalicylic Acid (x50 magnification), (b) Benzoic Acid (x50 magnification), (c) Nicotinic Acid (x75 magnification), (d) Paracetamol powder (x100 magnification) using 1mm scale

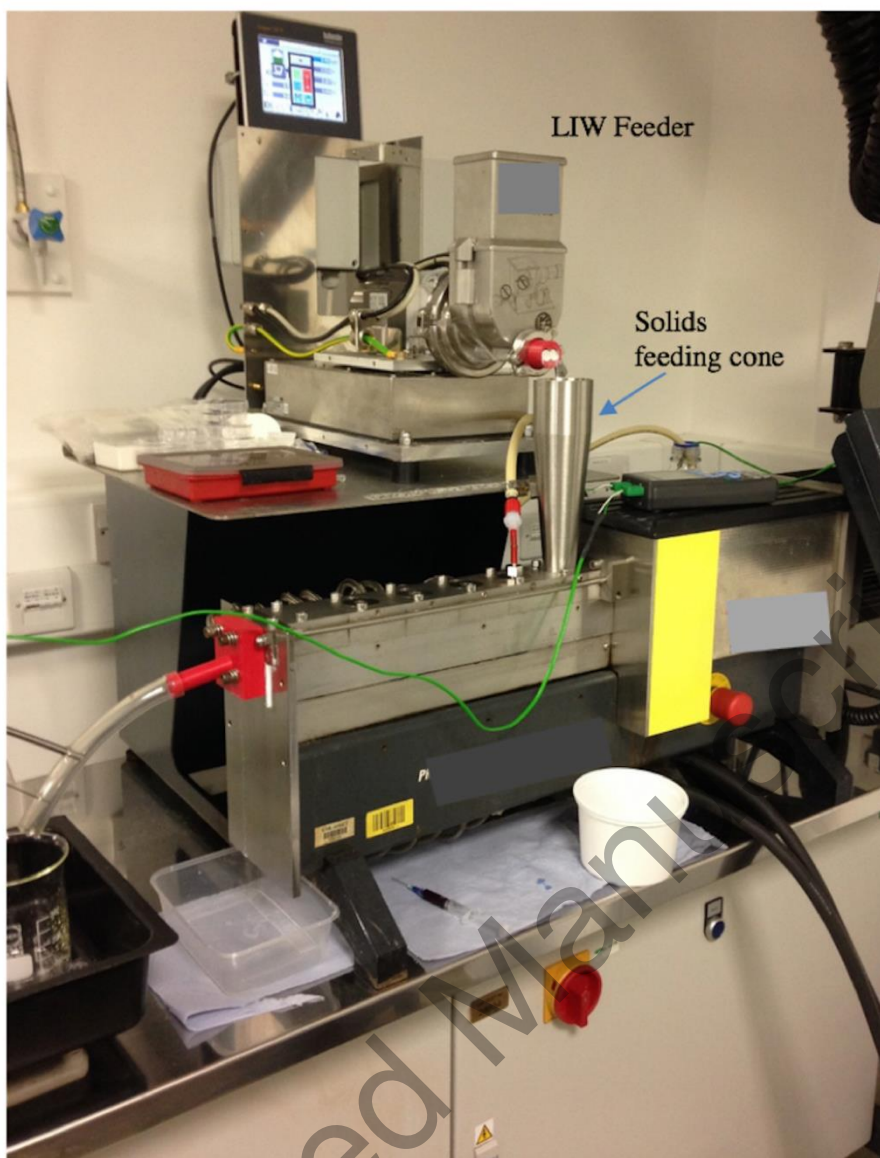Figure 3 Set up of stirred tank vessel for dissolution experiments

Figure 4 Set up of continuous twin screw extruder with LIW gravimetric feeder for dissolution experiments

Figure 5 Twin screws inside barrel of continuous twin screw extruder
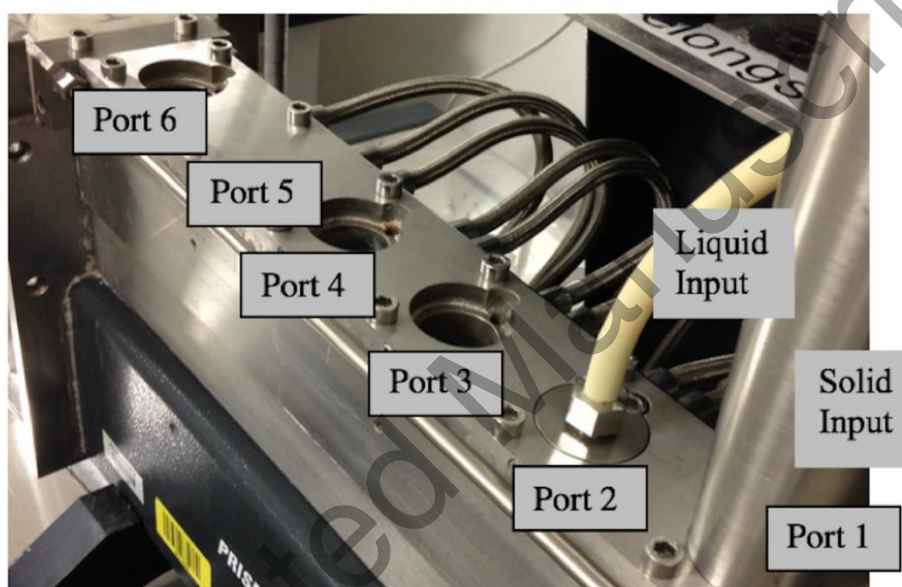
Figure 6 Barrel of twin screw extruder showing input port positions 1-6, port 5 has a

transferrable blank cover
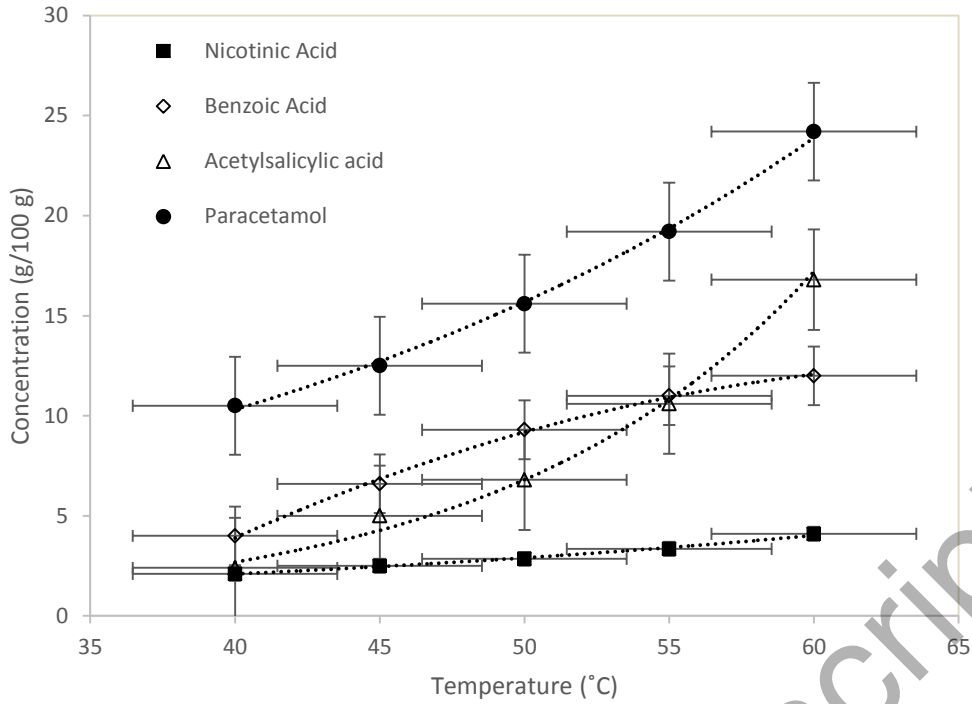
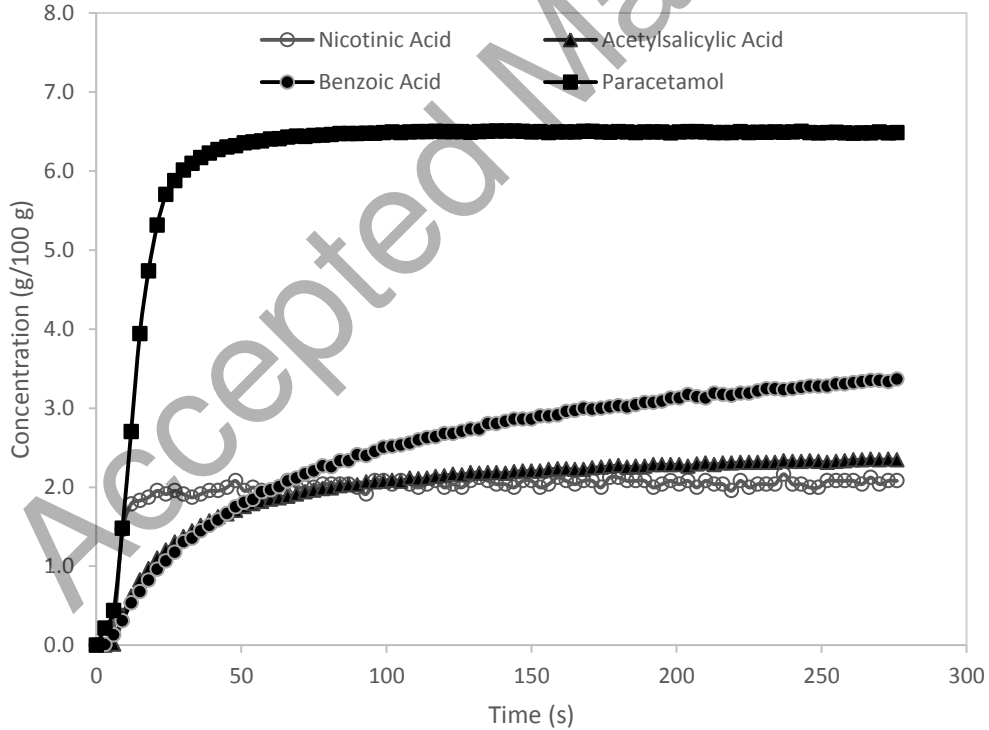Figure 7 Solubility of acetylsalicylic acid, benzoic acid, nicotinic acid and paracetamol in water/IPA (80:20)

Figure 8 Dissolution profiles of acetylsalicylic acid, benzoic acid, nicotinic acid and paracetamol in water/IPA (80:20) at 40˚C in a stirred tank vessel
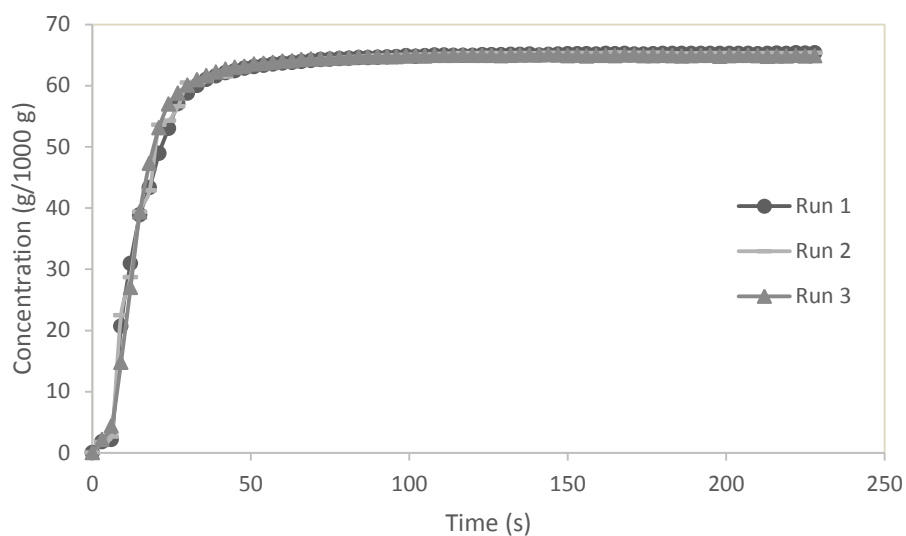
Figure 9 Dissolution profile of three experimental runs of powder paracetamol in water/IPA (80:20) in a stirred tank vessel (Temperature = 40°C, Mixing Speed = 750 rpm)
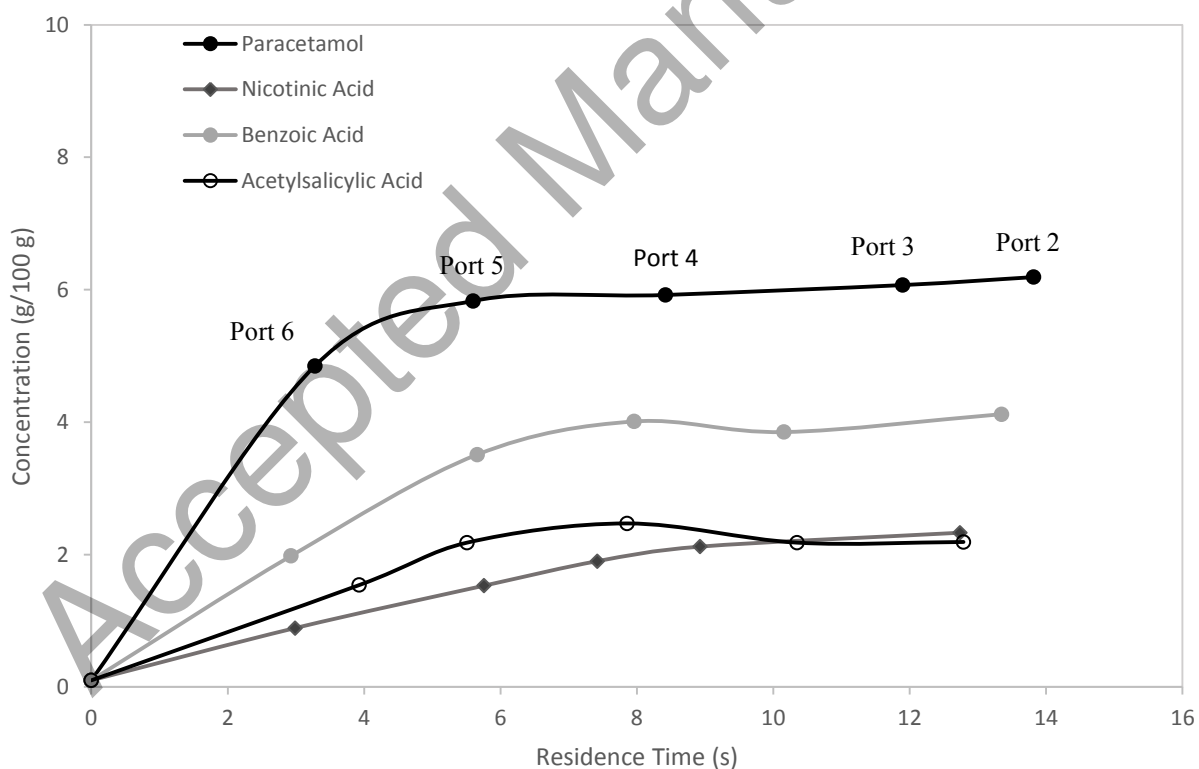

Figure 10 Concentration-time profile for acetylsalicylic acid, benzoic acid, nicotinic acid and paracetamol dissolution at exit of a twin screw extruder (Temperature = 40˚C, solid flow rate = 2.5 g min^{-1}, liquid flow rate = 40 g min^{-1})
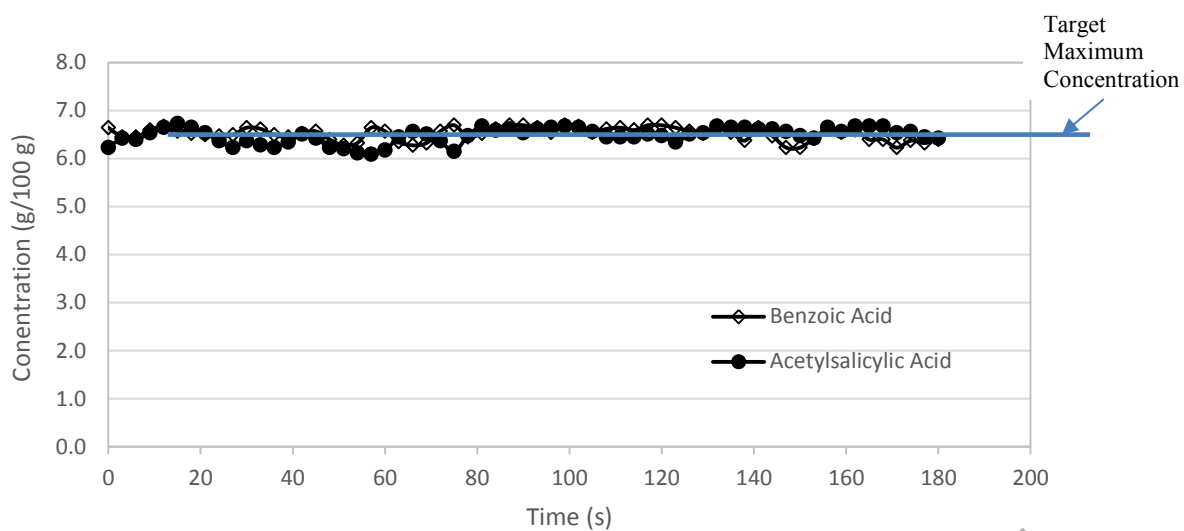
Figure 11 Concentration profile of benzoic acid and acetylsalicylic acid in water/IPA (80:20) at exit of a twin screw extruder (Temperature = 50˚C, solid flow rate = 2.5 g min^{-1}, liquid flow rate = 40 g min^{-1}

Table 1 Average particle sizes of acetylsalicylic acid, benzoic acid, nicotinic acid and paracetamol using laser diffraction

	Dx (10) (μm)	Dx (50) (μm)	Dx (90) (μm)
Benzoic Acid	813 ± 0.815	1460 ± 1.425	2510 ± 1.222
Acetylsalicylic Acid	338 ± 1.936	700 ± 3.865	1550 ± 2.995
Paracetamol Powder	12.6 ± 0.742	44.9 ± 2.570	124 ± 10.313
Nicotinic Acid	11.6 ± 2.115	30.9 ± 3.621	72 ± 4.497

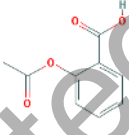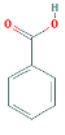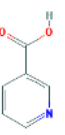Table 2 Chemical and physical properties of acetylsalicylic acid, benzoic acid, nicotinic acid and paracetamol
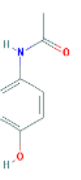
	Acetylsalicylic Acid	Benzoic Acid	Nicotinic Acid	Paracetamol
Hydrogen Bond Donor Count	1	1	1	2
Hydrogen Bond Acceptor Count	4	2	3	2
Topological Polar Surface Area (A^2)	63.6	37.3	50.2	49.3
Solubility in water at 25°C (mg ml^{-1})	4.6	2.9	18	15

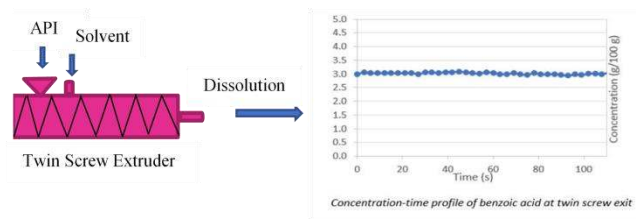Table 3 Solubility of acetylsalicylic acid, benzoic acid, nicotinic acid and paracetamol in water/IPA (80:20) at 40˚C

	Solubility (g/100 g)	% Error from Gravimetric measurement
Paracetamol	10.5	2.1
Benzoic acid	4.0	1.3
Acetylsalicylic acid	2.4	1.6
Nicotinic acid	2.1	1.9

Table 4 Dissolution rate constants for acetylsalicylic acid, benzoic acid, nicotinic acid and paracetamol in water/IPA (80:20) at 40˚C in a stirred tank vessel and a twin screw extruder

	Dissolution Rate constant, k (s^{-1})	Dissolution Rate constant, k (s^{-1})
	STV	TSE
Paracetamol	0.37	1.19
Nicotinic Acid	0.31	0.37
Benzoic Acid	0.18	0.72
Acetylsalicylic Acid	0.14	0.73

Table 5 Dissolution rate constants at fixed saturation level for acetylsalicylic acid, benzoic acid, nicotinic acid and paracetamol in water/IPA (80:20) at 40˚C in a stirred tank vessel and a twin screw extruder

			STV	TSE
	Saturation Level	% Saturation	Dissolution Rate constant, k (s^{-1})	Dissolution Rate constant, k (s^{-1})
Paracetamol	Undersaturated	67	0.37	1.19
Nicotinic Acid	Supersaturated	200	0.41	0.49
Benzoic Acid	Supersaturated	58	0.39	1.55
Acetylsalicylic Acid	Supersaturated	163	0.20	1.03

API   Solvent

Dissolution

Twin Screw Extruder

Concentration-time profile of benzoic acid at twin screw exit